

# Circulation

## Arrhythmia and Electrophysiology

JOURNAL OF THE AMERICAN HEART ASSOCIATION



**Stimulating Cardiac Muscle by Light : Cardiac Optogenetics by Cell Delivery**  
Zhiheng Jia, Virginijus Valiunas, Zongju Lu, Harold Bien, Huilin Liu , Hong-Zhang Wang,  
Barbara Rosati, Peter R. Brink, Ira S. Cohen and Emilia Entcheva  
*Circ Arrhythm Electrophysiol* 2011;4;753-760; originally published online August 9, 2011;  
DOI: 10.1161/CIRCEP.111.964247

Circulation: Arrhythmia and Electrophysiology is published by the American Heart Association. 7272  
Greenville Avenue, Dallas, TX 72514  
Copyright © 2011 American Heart Association. All rights reserved. Print ISSN: 1941-3149. Online ISSN:  
1941-3084

The online version of this article, along with updated information and services, is located  
on the World Wide Web at:

<http://circep.ahajournals.org/content/4/5/753.full>

Data Supplement (unedited) at:

<http://circep.ahajournals.org/content/suppl/2011/08/09/CIRCEP.111.964247.DC1.html>

Subscriptions: Information about subscribing to Circulation: Arrhythmia and Electrophysiology is online  
at  
<http://circep.ahajournals.org/site/subscriptions/>

Permissions: Permissions & Rights Desk, Lippincott Williams & Wilkins, a division of Wolters Kluwer  
Health, 351 West Camden Street, Baltimore, MD 21201-2436. Phone: 410-528-4050. Fax:  
410-528-8550. E-mail:  
[journalpermissions@lww.com](mailto:journalpermissions@lww.com)

Reprints: Information about reprints can be found online at  
<http://www.lww.com/reprints>

# Stimulating Cardiac Muscle by Light

## Cardiac Optogenetics by Cell Delivery

Zhiheng Jia, MS; Virginijus Valiunas, PhD; Zongju Lu, PhD; Harold Bien, MD, PhD;  
Huilin Liu, MS; Hong-Zhang Wang, PhD; Barbara Rosati, PhD; Peter R. Brink, PhD;  
Ira S. Cohen, MD, PhD; Emilia Entcheva, PhD

**Background**—After the recent cloning of light-sensitive ion channels and their expression in mammalian cells, a new field, optogenetics, emerged in neuroscience, allowing for precise perturbations of neural circuits by light. However, functionality of optogenetic tools has not been fully explored outside neuroscience, and a nonviral, nonembryogenesis-based strategy for optogenetics has not been shown before.

**Methods and Results**—We demonstrate the utility of optogenetics to cardiac muscle by a tandem cell unit (TCU) strategy, in which nonexcitable cells carry exogenous light-sensitive ion channels, and, when electrically coupled to cardiomyocytes, produce optically excitable heart tissue. A stable channelrhodopsin2 (ChR2)-expressing cell line was developed, characterized, and used as a cell delivery system. The TCU strategy was validated in vitro in cell pairs with adult canine myocytes (for a wide range of coupling strengths) and in cardiac syncytium with neonatal rat cardiomyocytes. For the first time, we combined optical excitation and optical imaging to capture light-triggered muscle contractions and high-resolution propagation maps of light-triggered electric waves, found to be quantitatively indistinguishable from electrically triggered waves.

**Conclusions**—Our results demonstrate feasibility to control excitation and contraction in cardiac muscle by light, using the TCU approach. Optical pacing in this case uses less energy, offers superior spatiotemporal control and remote access and can serve not only as an elegant tool in arrhythmia research but may form the basis for a new generation of light-driven cardiac pacemakers and muscle actuators. The TCU strategy is extendable to (nonviral) stem cell therapy and is directly relevant to in vivo applications. (*Circ Arrhythm Electrophysiol.* 2011;4:753-760.)

**Key Words:** optogenetics ■ channelrhodopsin2 ■ light-sensitive ion channels ■ cardiac ■ optical mapping

The simplest known opto-electric transducers in nature are a class of light-sensitive transmembrane proteins, best represented by bacteriorhodopsin, converting photons into transmembrane voltage through proton pumping. Since their discovery,<sup>1</sup> the prokaryote rhodopsins have been viewed as potential bioelectronics components<sup>2</sup> due to offered ultrafine spatiotemporal control by light. The latter is of equal interest in excitability control of eukaryotic cells. The cloning of Channelrhodopsin2 (ChR2) by Nagel, Hegemann, and colleagues<sup>3</sup> expanded the field beyond microorganisms. These ion channels provide excitatory current with relatively fast kinetics and can effectively trigger electric impulses (action potentials) in excitable cells. Since 2005,<sup>4,5</sup> numerous neuroscience applications in vitro and in vivo delineated a new research area, termed “optogenetics”<sup>4,6–12</sup>—the precise interrogation, stimulation, and control by light of excitable tissue, genetically altered to become light-sensitive.

---

### Editorial see p 598 Clinical Perspective on p 760

---

The use of optogenetics in other excitable tissues, for example, cardiac, skeletal, and smooth muscle, has been virtually nonexistent until very recently.<sup>13–15</sup> At the end of 2010, Bruegmann et al<sup>13</sup> combined viral expression of a ChR2 variant with a CAG promoter into mouse embryonic stem cells with targeted differentiation and purification of embryonic stem cell–derived cardiomyocytes for in vitro demonstration of optical pacing. They also generated transgenic mice with cardiac ChR2 expression, in which normal rhythm was perturbed by light pulses and focal arrhythmias were induced by long pulses. A transgenic zebra fish was used by Arrenberg et al<sup>14</sup> to spatially map the exact cardiac pacemaking region by structured illumination. At the same time, our group succeeded in developing the first nonviral strategy to optogenetics that does not rely on embryogenesis

---

Received March 14, 2011; accepted June 16, 2011.

From the Department of Biomedical Engineering (Z.J., H.B., E.E.), the Department of Physiology and Biophysics (V.V., Z.L., H.L., H.-Z.W., B.R., P.R.B., I.S.C., E.E.), and the Institute for Molecular Cardiology (B.R., P.R.B., I.S.C., E.E.); Stony Brook University, Stony Brook, NY.

The online-only Data Supplement is available at <http://circep.ahajournals.org/lookup/suppl/doi:10.1161/CIRCEP.111.964247/-DC1>.

Correspondence to Emilia Entcheva, PhD, HSC T18-30, Department of Biomedical Engineering, Stony Brook University, Stony Brook, NY, 11794-8181. E-mail [emilia.entcheva@sunysb.edu](mailto:emilia.entcheva@sunysb.edu)

© 2011 American Heart Association, Inc.

*Circ Arrhythm Electrophysiol* is available at <http://circep.ahajournals.org>

DOI: 10.1161/CIRCEP.111.964247

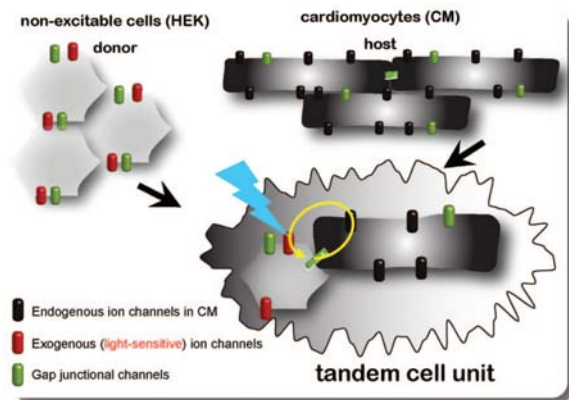


**Figure 1.** The functional “tandem cell unit” (TCU) concept of donor-host cells. Nonexcitable cells (eg, HEK cells) are transfected to express a light-sensitive ion channel (ChR2). When coupled through gap junctions to excitable cardiomyocytes (CM), they form an optically controllable functional TCU, that is, the CM will generate an action potential on light-triggered opening of the depolarizing ChR2 in the HEK cell.

and is applicable at the syncytial level—work presented in abstract form in 2010,<sup>15</sup> and reported in this article.

Unlike the brain, cardiac tissue is composed of densely packed, highly coupled cardiomyocytes, integrating electric and mechanical function. The heart’s electromechanical function requires synchrony of excitation waves for efficient global contraction, achieved by cell-cell coupling through gap junction channels formed by Connexin43 (Cx43) in the ventricular portion of the heart. We exploit the heart’s high coupling aspect to develop and validate a nonviral cell delivery system for expression of light-sensitive ion channels. Figure 1 illustrates the concept of a “tandem cell unit” (TCU), formed by a host cardiomyocyte and a nonexcitable donor cell, carrying exogenous ion channels, for example, ChR2. Biophysically, for this unit to be functional (to fire an action potential on light excitation), low-resistance coupling is needed for closing the local electric circuits. Our group has previously validated this concept for generation of a 2-cell pacemaking unit using cardiomyocytes and stem cells expressing a pacemaking ion channel.<sup>16</sup>

The TCU strategy, if proven successful, has potential safety advantages over viral delivery methods used in all prior optogenetics studies and may be applicable for study and treatment of cardiac rhythm disorders. In this work, we demonstrate the utility of optogenetics in the development of a more robust and energy-efficient solution for cardiac stimulation/actuation by (1) using a nonviral, cell delivery strategy to create optically excitable cardiac muscle, extendable to in vivo applications; (2) applying biophysical methods to validate the TCU strategy in cell pairs and in cardiac syncytium in vitro; and (3) demonstrating an all-optical sensing and actuation in a cardiac syncytium by combining optical stimulation with high-resolution optical mapping for quantification of wave properties under optical versus electric stimulation.

## Methods

As a proof-of-principle cell delivery system, we developed a stable HEK cell line expressing ChR2 and capable of Cx43-mediated

coupling<sup>16</sup> to cardiomyocytes to generate optically excitable cardiac tissue. The ChR2 plasmid, developed by the Deisseroth’s laboratory, was obtained from Addgene, Cambridge, MA (pcDNA3.1/hChR2(H134R)-EYFP), grown in replication-deficient bacteria, purified, and sequenced to confirm the published map. Transfection of the HEK293 cells (ATCC, Manassas, VA) was done with the use of Lipofectamine 2000 (Invitrogen, Carlsbad, CA), followed by 500  $\mu\text{g}/\text{mL}$  Geneticin (GIBCO Invitrogen) selection to achieve >98% expression. A detailed description of the Methods is available in the online-only Data Supplement.

We used whole-cell patch-clamp to confirm ChR2-mediated inward current inducible by pulses of blue light (470/40 nm) in the developed cell line. The TCU concept was validated using a dual-patch technique<sup>16</sup> in cell pairs of adult canine cardiomyocytes (CM), isolated as described before,<sup>16</sup> and HEK-ChR2 cells, as well as in coculture of neonatal rat CM<sup>17–19</sup> with ChR2-expressing HEK cells at initial plating ratio 100:1 or 45:1. Without explicit suppression of proliferation, within the 2 to 3 days to experiments, the effective ratio was severalfold lower. These in vitro syncytia were used for tissue-level optical mapping of excitation and contraction. In some experiments, carbenoxolone, a gap-junction uncoupler, was applied as described to probe the role of cellular coupling in the TCU approach.

Electric stimulation was provided through Platinum electrodes, driven by a computer-controlled stimulator. For most experiments, optical stimulation was through the dish bottom, by focused light from a blue LED (470 nm, 1.35 cd, 20 mA) or a fiberoptics-coupled high-power blue LED (470 nm, 1.6 A), connected to the TTL output of a second computer-driven stimulator.

Optical tracking of excitation waves was done using Rhod-4, a calcium-sensitive probe, with excitation at 525/40 nm and emission at 610/75 nm to avoid interference of the stimulation light with the dye’s excitation spectrum. A nonconventional distributed tangential illumination was used to accommodate optical stimulation and for superior contrast. Emitted light was collected through high-NA optics and a fast intensified CMOS camera. Records of contractility were done with Hamamatsu Imagem EMCCD camera on a confocal Olympus FluoView FV1000.

Data from multiple samples are presented, as indicated, using standard deviation, standard error of the mean, or 95% confidence intervals. Statistical testing for functional data on propagation was done in Matlab using a standard 2-way ANOVA, followed by a Tukey-Kramer correction for multiple comparisons; probability values are listed for all comparisons. Normality of the distributions was confirmed by Kolmogorov-Smirnov test in Matlab, except for data on coupling in cell pairs, in which nonparametric population statistics was applied (median and interquartile range). Curve-fitting was done also in Matlab, using the robust nonlinear least-squares fit method, with prespecified equations for the desired curve types, for example, a sigmoidal curve or exponential decay.

## Results and Discussion

### Development and Characterization of a Cell Delivery System for Nonviral Optogenetics

To validate the TCU strategy for cardiac optogenetics, as a proof of principle, we developed a stable HEK cell line expressing a variant of ChR2. Figure 2A through 2E illustrates the properties of such donor cell line. Preserved expression and functionality were established for the HEK-ChR2 cell line after multiple freeze-thaw cycles and multiple passages (passages 2 to 30 were used for functional experiments, Figure 2A). Successful expression is possible in other nonexcitable cell types, including mesenchymal stem cells (online-only Data Supplement Figure I), which may yield more clinically relevant cell delivery systems.

Confirmation of ChR2 functionality was done by whole-cell voltage clamp. Quantification of the steady-state light-sensitive ion current in single HEK-ChR2 cells (Figure 2B and 2C)

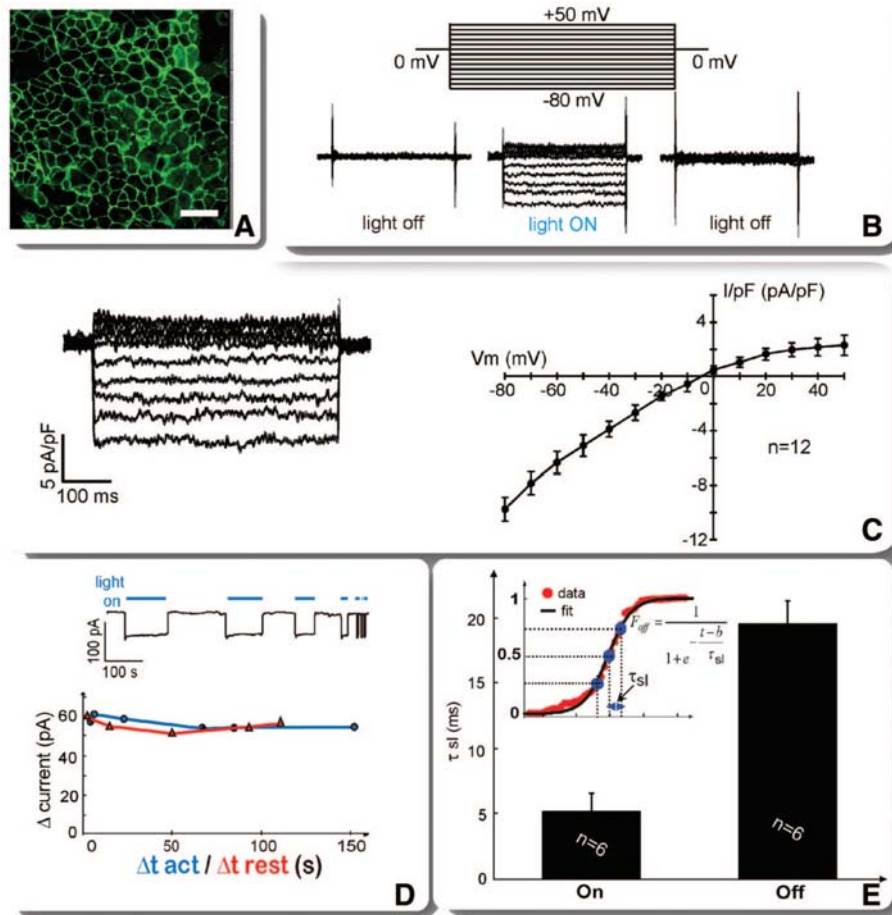


**Figure 2.** Development and functional characterization of a cell delivery system for light-sensitive ion channel (ChR2). **A**, Stable HEK-ChR2 cell line: Shown is EYFP-reported ChR2 expression in the 10th passage after transfection and purification; scale bar is 50 μm. **B**, Voltage-clamp test protocol and example traces for quantification of the steady-state ChR2 current in single HEK-ChR2 cells with 500-ms voltage pulses in the range (−80 to +50mV) with and without excitation light for ChR2 on (470 nm, 0.24 mW/mm<sup>2</sup>). **C**, Example curves for the light-sensitive component after subtraction of current in dark and the resultant average current-voltage (I-V) relationship for n=12 cells, cell capacitance 43.3±7.5 pF; data are presented as mean±SD. **D**, Magnitude of the light-triggered current does not depend on the duration of rest (Δt rest) or activation (Δt act), thus indicating relatively fast deactivation in the examined range. Holding potential is −80 mV. **E**, Kinetics of activation (on) and deactivation (off), quantified by a τ<sub>sl</sub> parameter in the sigmoid curve fits to the light-controlled current transitions (see inset); bar graphs represent mean±SEM.

revealed that the channel is closed and noncontributing during dark periods regardless of transmembrane voltage and has a mildly inwardly rectifying current-voltage (I-V) relationship when blue light is applied. Overall, significantly higher steady-state current densities were seen in our donor cells at all voltages in the I-V relationship, even at the low irradiance used here (0.24 mW/mm<sup>2</sup>), compared with previously reported light-induced ChR2 current in HEK cells,<sup>20</sup> *Caenorhabditis elegans* muscle cells,<sup>10</sup> or in cardiomyocytes.<sup>13</sup> For example, for comparable irradiance levels, at holding potential of −40 mV, about 20-times-higher steady-state current densities were measured in our donor cells compared with ventricular myocytes from a transgenic mouse expressing ChR2.<sup>13</sup> These data confirm high expression levels and/or functionality of ChR2 in the developed cell delivery system, important for optimizing light stimulation parameters.

Recent comprehensive characterization of ChR2 current kinetics indicates fast activation (<5 ms), deactivation (<10

ms), and inactivation (<50 ms),<sup>20</sup> thus making it suitable as excitatory (action potential-generating) current for cardiomyocytes during external optical pacing at relevant frequencies (5 to 12 Hz for rodents, 1 to 3 Hz for humans). Indeed, our kinetics characterization (Figure 2D and 2E) estimates the activation and deactivation time constants for ChR2-mediated current in the ms range. Therefore, suitable rates for cardiac pacing are attainable even without genetic modifications, as previously done for neural applications, in which faster optogenetic tools in conjunction with much shorter action potentials allowed for pacing rates up to 200 Hz.<sup>9</sup>

In contrast to the robust expression of ChR2 in HEK cells, much lower yield was seen when directly transfecting cardiomyocytes with ChR2 with the use of nucleofector electroporation. This prevented direct synthesis of a large-scale ventricular syncytium from ChR2-expressing myocytes. Nevertheless, individual ChR2-expressing neonatal rat ventricular myocytes were excitable and contract-

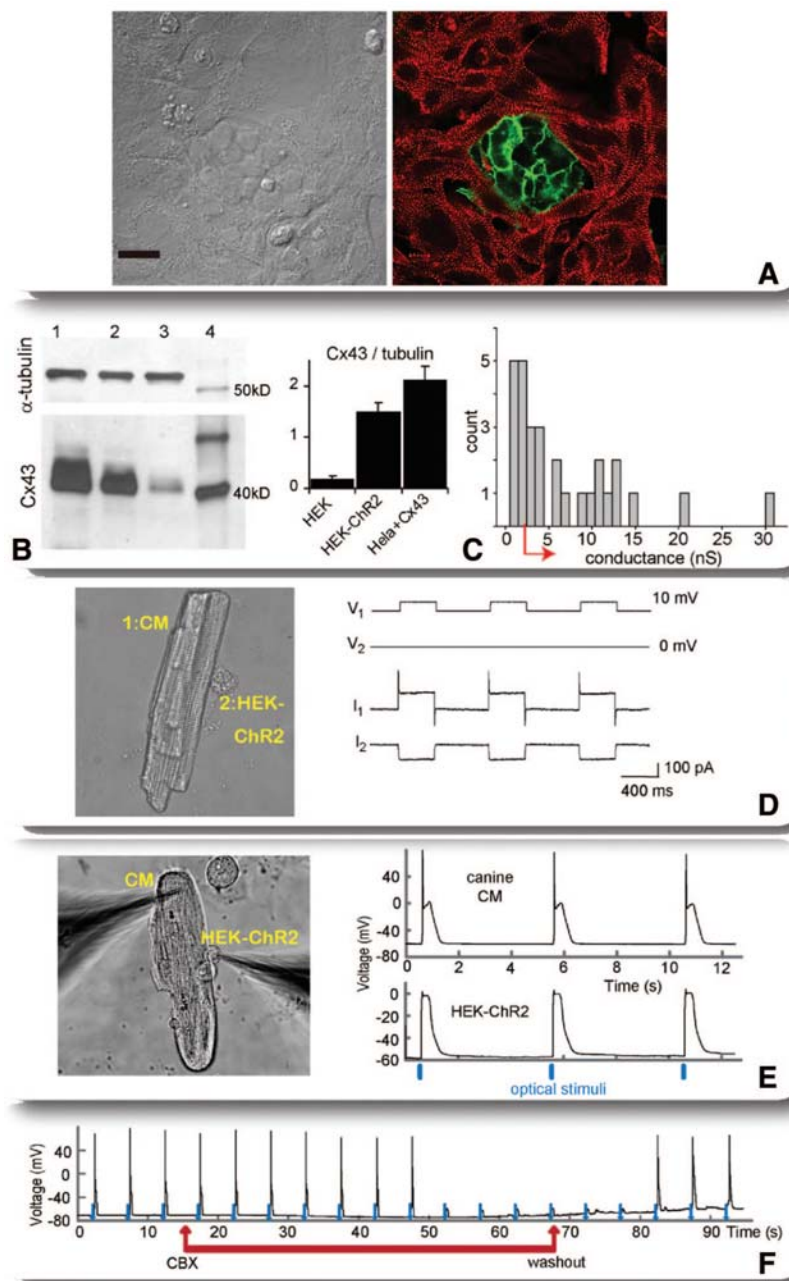


**Figure 3.** Implementation and validation of the “tandem cell unit” (TCU) concept for neonatal rat cardiomyocytes (CM) and adult canine CM coupled to HEK+ChR2 cells. **A**, Phase and fluorescence images of neonatal rat CM and HEK-ChR2 coculture. Immunostaining in red for  $\alpha$ -actinin (CMs), green is EYFP-ChR2-expressing HEK cells, typically forming small clusters as shown. Scale bar is 20  $\mu$ m. **B**, Western blot for Connexin43 (Cx43) and  $\alpha$ -tubulin (at 55 kD) in the cell delivery system (HEK-ChR2; **column 2**); **column 1** shows a positive control of stably transfected HeLa-Cx43 cells; **column 3** shows parental HEK cells without ChR2; **column 4** shows the ladder—MagicMark bands in kDa; Normalized (Cx43/tubulin) expression is provided for 4 gels (mean $\pm$ 95% confidence interval). **C**, Histogram of measured coupling conductances in TCUs of canine CMs and HEK-ChR2 cells (n=31, median value of 4 nS and interquartile range of 2 to 11 nS); **red arrow** indicates coupling levels allowing optical excitability of the TCUs. **D**, Dual whole-cell voltage clamp of a TCU adult canine ventricular CM (1) and HEK-ChR2 cell. (2) Voltage steps ( $V_1=10$  mV, 0.4 seconds) applied to the canine CM (cell 1) induced junctional currents ( $I_2$ ) in this cell pair (estimated g.j., conductance of 11 nS). **E**, Action potentials in a cell pair (canine CM and HEK-ChR2 cell, phase image on the left) in response to optical pacing (0.13 mW/mm<sup>2</sup>, 10-ms pulses). Due to coupling, the HEK cell exhibits a low-pass-filtered version of the CM-generated action potentials. **F**, Action potentials in a cell pair (canine CM and HEK-ChR2 cell) in response to continuous optical pacing before, during, and after washout of uncoupler carbenoxolone (CBX).

ing when optically stimulated and quiescent otherwise (online-only Data Supplement Movie 1).

### Validation of the TCU Strategy for Cardiac Excitation

The TCU approach for cardiac optogenetics, that is, inscribing light sensitivity into cardiomyocytes and cardiac tissue without their direct genetic modifications, was validated in cell pairs of CM and HEK-ChR2 cells as well as in a synthesized large-scale cardiac syncytium. ChR2-expressing donor cells were most often found to aggregate in small clusters among the neonatal CMs rather than disperse as single cells (Figure 3A). The donor cells expressed a significant amount of Cx43, as confirmed by a

Western blot (Figure 3B). Interestingly, substantially more Cx43 protein was seen in the HEK-ChR2 cells compared with the parental cell line without ChR2, an observation that warrants further investigation.

Functional response of TCUs to optical stimulation was first confirmed in cell pairs of adult canine CM and HEK-ChR2 cells using dual-clamp to estimate coupling (Figure 3C and 3D) and to record light-triggered action potentials in the cardiomyocytes (Figure 3E and 3F). A histogram of measured coupling in spontaneously formed cell pairs (n=31) of canine CM and HEK-ChR2 over 48-hour period is shown (Figure 3C). A robust response was seen in a wide range of coupling values spanning an order of magnitude, starting as low as 1.5

nS. Interestingly, a similar low critical coupling value (1.5 to 2 nS), below which TCU functionality failed, was found previously in the generation of a 2-cell pacemaking unit by a donor cell carrying HCN2 (a gene encoding for the pacemaking current  $I_p$ ) and a cardiomyocyte.<sup>16</sup> Extreme uncoupling abolished the light sensitivity of the myocytes in the TCUs—values below 1.5 nS and pharmacological uncoupling with cabenoxolone provided further proof for gap junctions' critical role in the TCU functionality for neonatal rat and for adult canine myocytes (Figure 3F and online-only Data Supplement Movie 2).

In a functional TCU pair, the cardiomyocytes generated normal action potentials on stimulation by blue light (470 nm, 0.13 mW/mm<sup>2</sup>, 10-ms pulses; Figure 3E), indistinguishable from electrically triggered ones. The donor cell's membrane potential followed passively by a low-pass filtered version of an action potential (Figure 3E). In a spatially extended (several centimeters), 2-dimensional cardiac syncytium of randomly mixed neonatal rat CMs and HEK-ChR2 (45:1 initial plating ratio), robust synchronous contractions were registered on stimulation by blue light 2 to 3 days after plating (online-only Data Supplement Movie 3).

### Wave Properties of Cardiac Syncytium in Response to Optical Versus Electric Stimulation

Synthesized optically excitable cardiac tissue was then subjected to further functional testing. Synchronized wave propagation is essential for the heart's normal functionality and efficient mechanical contraction; lethal arrhythmias occur when the generation or propagation of these excitation waves is altered (failure to initiate, abnormal propagation velocity and/or path). Accordingly, we have developed an ultra-high-resolution optical mapping system<sup>18,19</sup> to dissect cardiac wave propagation during external pacing or arrhythmic activity over a centimeter scale (>2 cm) with subcellular resolution (22  $\mu$ m/pix) at 200 fps, using fast voltage and calcium-sensitive dyes.<sup>18</sup> This optical mapping system was made compatible with simultaneous optical excitation (Figure 4A), so that excitation light for the fluorescence measurements did not induce ChR2 excitation and ChR2 excitation did not interfere with the measurements. Although mapping was done with Rhod-4, a calcium-sensitive fluorescent dye, suitable voltage-sensitive probes with similar spectral properties can also be used, for example, di-4 or di-8-ANEPPS.<sup>18</sup> In normal pacing conditions, cardiac calcium transients are an excellent surrogate for action potentials, and calcium dyes outperform voltage-sensitive dyes in signal-to-noise ratio.

Optical mapping of propagating waves triggered by localized electric and optical stimulation in the same sample revealed similar conduction velocities and calcium transient morphologies, thus confirming equivalent triggering abilities for both modes of stimulation (Figure 4B through 4E and online-only Data Supplement Movie 4). Pure cardiomyocyte cultures and cocultures of cardiomyocytes and HEK cells without ChR2 served as controls. At the mixing ratios used here, the presence of HEK cells, with or without ChR2, did not alter the recorded calcium transients (Figure 4C and 4D;  $P=0.36$  with ChR2,  $P=0.44$  without ChR2). However, the

mixing ratio was a significant factor ( $P<0.0001$ ) in modulating CV, as revealed by a 2-way ANOVA, that is, about 30% drop in CV was seen at initial plating ratios of 45:1 (CM:HEK), whereas a ratio of 100:1 led to a smaller (nonsignificant,  $P=0.06$ ) reduction (Figure 4E). The presence of ChR2 did not contribute as a significant factor in CV modulation ( $P=0.16$ ), even though a slight trend to a decrease was seen. Further titration (higher mixing ratios) and/or localized spatial distribution are likely to minimize these effects. Electric and optical pacing in light-sensitive samples (CM:HEK+ChR2) resulted in identical wave propagation properties. The controls (CM only and CM+HEK without ChR2) were quiescent and never produced excitation in response to light triggers.

The response of the syncytium to optical excitation was captured by constructing a strength-duration curve, describing minimum irradiance over a range of pulse duration values for a point excitation of the 2D syncytium (2-mm fiberoptic-coupled controllable LED, Figure 4F). The fitted curve revealed a particularly low minimal irradiance levels (average rheobase<sup>21</sup> for excitation of about 0.05 mW/mm<sup>2</sup>)—at least an order of magnitude lower than previously shown values for optical stimulation of ventricular or atrial tissue.<sup>13</sup> Within the tested diameter for light delivery, macroscopic excitability remained uniform across the tissue. However, we anticipate that donor cell clustering (Figure 3A) must be addressed to achieve maximal spatial resolution of excitation, down to the single-cell level.

Considering the electromechanical nature of cardiomyocytes, we also show direct light-triggered muscle contraction, confirming intact excitation-contraction coupling in single myocytes or hybrid cardiac tissue (Figure 4G and online-only Data Supplement Movies 1 to 3). This demonstration of mechanical response triggered by light-sensitive ion channels suggests possible development of light-driven actuators with efficient energy transfer and illustrates the feasibility for direct optogenetic control in other muscles.

### Energy Needs in Cardiac Optogenetics

Previous studies in neuroscience have reported optical energies used to excite single neurons or brain tissue<sup>4,6,22</sup> in a wide range of high values (approximately 8 to 75 mW/mm<sup>2</sup>). The well-coupled spatially extended cardiac tissue was expected to present higher load for optical stimulation, thus possibly requiring even higher irradiance values. Yet, surprisingly, in Bruegmann et al's study,<sup>13</sup> significantly lower light levels (0.5 to 7 mW/mm<sup>2</sup>) were sufficient to optically stimulate cardiac tissue in vitro or in vivo for a wide range of pulse durations.

In our TCU approach, during optical pacing in the cell pairs or in the 2-dimensional cardiac syncytium, we measured irradiance at 470 nm as low as 0.006 mW/mm<sup>2</sup>. The strength-duration curve (Figure 4F) further corroborated low irradiance needed across pulse durations. Interestingly, this is much lower than reported for neuroscience applications and about 1 to 2 orders of magnitude lower than previously reported values for cardiac excitation in cells and tissue<sup>13</sup> for comparable pulse durations. The significantly lower optical energy needed in our study can be explained, at least

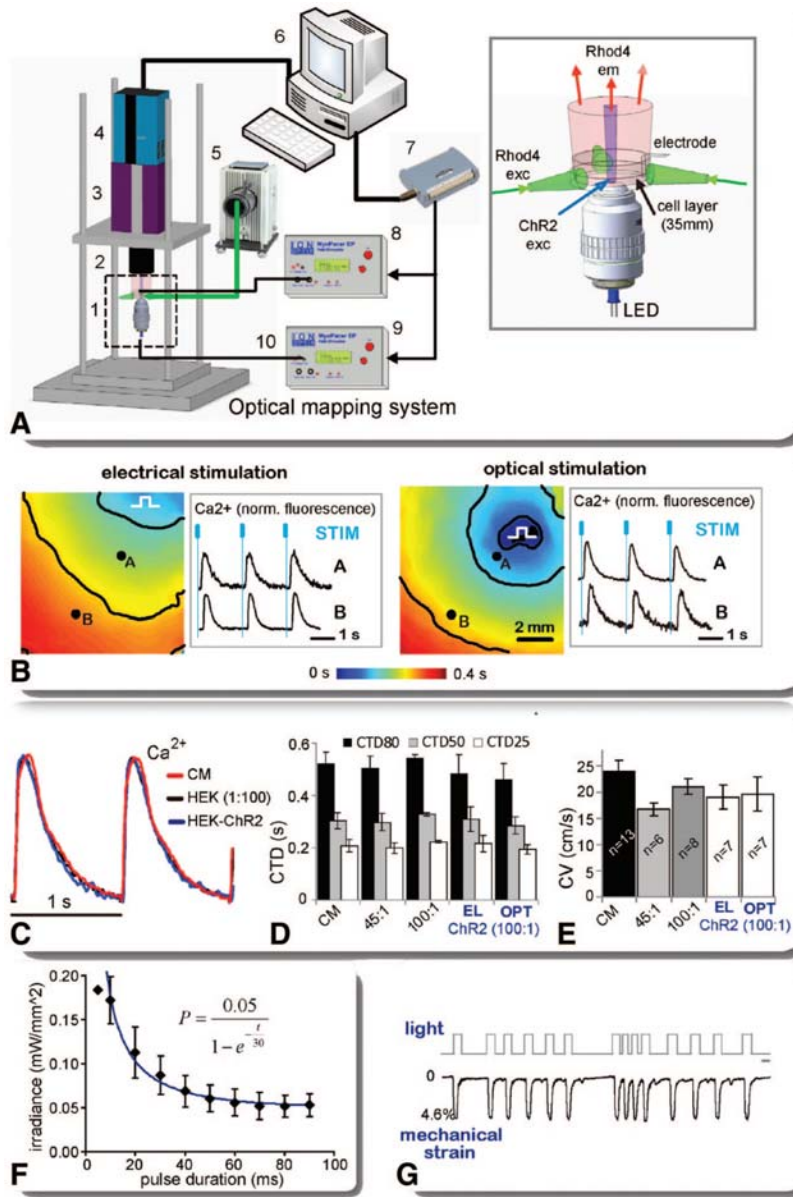


**Figure 4.** Optical control of cardiac tissue function over space-time: Light-triggered excitation waves and light-triggered contractions. **A**, Experimental setup for ultra-high-resolution, high-speed optical imaging and optical control of cardiac excitation: 1, Experimental chamber with tangential light illumination for calcium imaging, focused LED illumination on a moveable stage for light-sensitive ion channel (ChR2) excitation (see inset on the right); 2, high-NA optics for high-resolution macroscopic imaging; 3, Gen III MCP intensifier; 4, pco1200hs CMOS camera; 5, light source, excitation filter, and optical light guides for tangential excitation; 6, computer system and software for data acquisition and control of electric and optical stimulation; 7, interface for stimulation control; 8, controllable stimulator for electric pacing (analog output); 9, controllable stimulator for optical pacing (TTL output); 10, LED for ChR2 excitation, driven by the TTL stimulator output. **B**, Activation maps in a cardiac monolayer by electric and optical pacing at 0.5 Hz. Color represents time of activation; isochrones are shown in black at 0.15 seconds. Calcium transient traces in response to electric or optical stimulation are shown from 2 locations (A and B), normalized fluorescence. Blue marks indicate time of stimulation (electric pulses were 10 ms; optical, 20 ms each). **C**, Normalized  $Ca^{2+}$  transients from CM monolayer (red), CM:HEK (black) and CM:HEK+ChR2 coculture 100:1 (blue) at 1-Hz pacing. **D**, Quantification of calcium transient duration (CTD)—CTD25, CTD50, and CTD80 for pure cardiomyocyte (CM) monolayer, 45:1 and 100:1 CM:HEK, as well as 100:1 CM:(HEK+ChR2) coculture under electric and optical pacing at 1 Hz. **E**, Comparison of conduction velocity (CV) among the same 5 groups as in (D); for D and E, optical pacing was at irradiance of 0.01 to 0.04 mW/mm<sup>2</sup>, 50-ms pulses; data are shown as mean±95% confidence interval; listed number of samples applies to both; **F**, Strength-duration curve (along with the equation for the fitted curve) obtained for optical pacing in cocultures (100:1 CM:HEK ratio) at 30°C (n=8, mean±SEM). **G**, Example contractility recording from optically driven CM+HEK+ChR2, displacement normalized to cell length. Scale bar is 1 second.

partially, by the superior light sensitivity of the donor cells as seen in the higher ChR2 current densities (Figure 2C). Further differences when compared with optical excitation of ventricular and atrial tissue may stem from dimensionality (2D in the present study versus 3D<sup>13</sup>).

It is important to note that in contrast to a previous study,<sup>13</sup> no (proarrhythmic) reexcitations were observed during longer stimulation pulses (up to 1 second) at our low illumination intensities, close to the rheobase of the strength-duration curve. This low light intensity is an important factor in minimizing heat-related effects, phototoxicity, and in considering future implantable devices.

An interesting question concerns comparison of energy needed for electric versus optical pacing. In our system, energy needed for suprathreshold stimulation of 2-dimensional cardiac syncytium can be estimated as follows:

For typical electric pacing (5 V, 0.2 A, 0.01-second pulses), we obtain 10 mJ. For optical stimulation with an LED (5 V, 0.02 A, 0.01- to 0.05-second pulses), we obtain 1 to 5 mJ. Considering the possibility for optimization of light focusing as well as the active development of more efficient light-emitting diodes (more lumens per Watt), it is likely that optical stimulation may be more energy efficient than its electric counterpart. Because pacemaking (unlike cardioversion) is a topologically simple problem, that is, a spatially localized (light-sensitive) cell ensemble can be used, the TCU strategy may prove particularly valuable in pursuing potential clinical applications, given the above energy considerations. However, the challenges of achieving efficient light delivery to a densely packed tissue, such as the myocardium, should not be underestimated, and ultimately in vivo testing is needed.

### Potential Benefits of the TCU Strategy and In Vivo Considerations

When comparing the TCU strategy with the direct expression of ChR2 in native myocytes (mostly by viral methods), several important differences are worth mentioning (see also online-only Data Supplement Figure II): (1) the donor (D) cells are nonexcitable and typically do not have major repolarizing currents, that is, the ChR2 inward current is their main current, unlike native CMs; (2) the D-cells have higher membrane impedance at rest due to smaller/negligible inward rectifier,  $I_{K1}$ , and typically have a more depolarized resting potential; and (3) compared with CM-CM coupling, the D-CM coupling is typically somewhat reduced. We ask the question: What factors in the TCU approach affect the ease of excitation and how is the TCU response to light different than the response of a homogeneous myocardial tissue with direct expression of ChR2?

For a spatially extended tissue, when the cell pair (TCU) is connected to some “load” of excitable cells (CMs), the system can be abstracted to a Source-Neighbor-Load (S-N-L) triad for easier analysis. A simplified equivalent circuit of such a triad is presented in online-only Data Supplement Figure II, D, and analysis is provided in detail in the online-only Data Supplement.

The main results of this analysis (online-only Data Supplement Figure II, D) are that the ease of optical excitation will improve with (1) higher membrane impedance for the source/donor cell (as seen for a D versus CM source cell), since that makes it closer to an ideal current source, and a higher excitation current is available for the neighboring CMs for the same light-induced current in the source, (2) lower membrane impedance of the immediate CM neighbors, determined by their  $K^+$  conductance, and (3) better S-N coupling but reduced coupling in the load and reduced overall impedance of the load. It is important to note that for spatially dispersed donor cells, as here, the S-N coupling in the S-N-L triad plays a dual role, that is, it affects both the S-N charge transfer and the equivalent “load” presented by the tissue. Since the two have opposite effects on the ease to excite, there may be an optimal D-CM coupling for excitation via the TCU strategy.

Having a dedicated donor cell may also provide additional benefits by allowing donor cell optimization independent of the properties of the target tissue, for example, maximizing the light sensitivity by achieving high current densities in the donor with proper cellular environment for the function of the ChR2 channels.

The presented cell delivery method can be viewed as an easy and accessible research tool for basic studies *in vitro*. Its feasibility for potential *in vivo* cardiac pacing is supported by prior relevant studies, including one using mesenchymal stem cells with a depolarizing current,  $I_p$ , in a canine heart,<sup>23</sup> in which the cells’ survival and functionality was demonstrated for at least several weeks. In that study, about 0.7 million cells were delivered, 40% of them carrying the HCN2 gene, encoding for an  $I_p$ -like current, expressed at comparable densities to our ChR2 current.<sup>24</sup> The cell number needed for localized excitation can be further inferred from considerations of tissue properties, that is, estimates of “liminal

length” (the minimum size of tissue capable of exciting the rest),<sup>25,26</sup> which in some cases can be derived from the strength-duration curve. Recent estimates by computer simulations of a related problem—localized generation of early or delayed afterdepolarizations<sup>27</sup>—yielded about 0.7 million cells in a cluster required for maximum load (worst case scenario), that is, 3D highly coupled ventricular myocardium. With decreased coupling and other load reductions, this cell number also decreased. Because we did not perform experiments with a confined cell region in 2D, it is difficult to directly relate to these estimates. Nevertheless, these studies support the general feasibility of *in vivo* cell delivery for optical pacing by the TCU approach, provided that an appropriate light delivery solution is found. Optimizing the light sensitivity of the donor cells partially alleviates these challenges. Compared with pacing, cardioversion and defibrillation are topologically more complicated problems due to their inherent spatial component and requirement for spatially distributed light sensitivity and light delivery. Stability and long-term functionality of ChR2 *in vivo* have not been studied rigorously, but preliminary data from ChR2 use in primate brains over several months are promising in terms of persistence and lack of toxicity.<sup>28</sup>

### Conclusions

In summary, our study highlights the utility of optogenetics for cardiac applications by using a strategy inspired by the specific properties of cardiac tissue, that is, high cell-cell coupling. The optogenetic approach offers high spatiotemporal resolution for precise interrogation and control of excitation, seemingly without interfering with essential cardiac tissue properties. Therefore, it presents a new versatile actuation tool in cardiac research for dissection of arrhythmias. Furthermore, cardiac optogenetics, based on the TCU strategy presented in the present study, may evolve in a more translational direction and lead to a new generation of optical pacemakers and potentially cardioverter/defibrillators. The feasibility of this is supported by several critical features of the method presented in the present study: (1) desirable pacing rates achievable with the current kinetics of ChR2; (2) finer control of excitation and repolarization in shaping cardiac action potentials and potentially in terminating arrhythmias is possible by a combination of light-sensitive ion channels providing outward current<sup>7-8</sup> and ChR2; (3) the cell delivery platform demonstrated here may offer a safer alternative to viral delivery for *in vivo* applications; (4) optical fibers are inherently more biocompatible than metal electrode leads for *in vivo* pacing; and (5) preliminary energy estimates point to potential fold improvements in energy consumption with optical versus electric pacing—important for extending battery life in implantable devices.

### Acknowledgments

We thank Jacqueline Guenther for cardiac cell culture preparation, Joan Zuckerman for canine cell isolation, Yuanjian Guo for canine mesenchymal stem cell isolation, Laima Valiuniene for heterologous cell culture with canine myocytes, Chris Gordon for Western blots, and Qinghong Yan, for help with expansion and purification of the ChR2 plasmid.



### Sources of Funding

We acknowledge support from NIH-NIGMS-funded Systems Biology Center in New York State (GM071558, Dr Entcheva), NLHBI grant HL094410 (Dr Cohen), NIGMS grant RO1GM088181 (Dr Valiunas), and a grant from the Institute for Molecular Cardiology at Stony Brook University (Dr Entcheva).

### Disclosures

None.

### References

- Oesterhelt D, Stoekenius W. Rhodopsin-like protein from the purple membrane of halobacterium halobium. *Nat New Biol*. 1971;233:149–152.
- Vsevolodov NN. *Biomolecular Electronics: An Introduction Via Photosensitive Proteins*. Boston: Birkhauser; 1998.
- Nagel G, Szellas T, Huhn W, Kateriya S, Adeishvili N, Berthold P, Ollig D, Hegemann P, Bamberg E. Channelrhodopsin-2, a directly light-gated cation-selective membrane channel. *Proc Natl Acad Sci U S A*. 2003;100:13940–13945.
- Boyden ES, Zhang F, Bamberg E, Nagel G, Deisseroth K. Millisecond-timescale, genetically targeted optical control of neural activity. *Nat Neurosci*. 2005;8:1263–1268.
- Li X, Gutierrez DV, Hanson MG, Han J, Mark MD, Chiel H, Hegemann P, Landmesser LT, Herlitze S. Fast noninvasive activation and inhibition of neural and network activity by vertebrate rhodopsin and green algae channelrhodopsin. *Proc Natl Acad Sci U S A*. 2005;102:17816–17821.
- Wang H, Peca J, Matsuzaki M, Matsuzaki K, Noguchi J, Qiu L, Wang D, Zhang F, Boyden E, Deisseroth K, Kasai H, Hall WC, Feng G, Augustine GJ. High-speed mapping of synaptic connectivity using photostimulation in channelrhodopsin-2 transgenic mice. *Proc Natl Acad Sci U S A*. 2007;104:8143–8148.
- Chow BY, Han X, Dobry AS, Qian X, Chuong AS, Li M, Henninger MA, Belfort GM, Lin Y, Monahan PE, Boyden ES. High-performance genetically targetable optical neural silencing by light-driven proton pumps. *Nature*. 2010;463:98–102.
- Han X, Boyden ES. Multiple-color optical activation, silencing, and desynchronization of neural activity, with single-spike temporal resolution. *PLoS One*. 2007;2:e299.
- Gunaydin LA, Yizhar O, Berndt A, Sohal VS, Deisseroth K, Hegemann P. Ultrafast optogenetic control. *Nat Neurosci*. 2010;13:387–392.
- Nagel G, Brauner M, Liewald JF, Adeishvili N, Bamberg E, Gottschalk A. Light activation of channelrhodopsin-2 in excitable cells of *Caenorhabditis elegans* triggers rapid behavioral responses. *Curr Biol*. 2005;15:2279–2284.
- Airan RD, Thompson KR, Fenno LE, Bernstein H, Deisseroth K. Temporally precise in vivo control of intracellular signalling. *Nature*. 2009;458:1025–1029.
- Huber D, Petreanu L, Ghitani N, Ranade S, Hromadka T, Mainen Z, Svoboda K. Sparse optical microstimulation in barrel cortex drives learned behaviour in freely moving mice. *Nature*. 2008;451:61–64.
- Bruegmann T, Malan D, Hesse M, Beiert T, Fuegemann CJ, Fleischmann BK, Sasse P. Optogenetic control of heart muscle in vitro and in vivo. *Nat Methods*. 2010;7:897–900.
- Arrenberg AB, Stainier DY, Baier H, Huisken J. Optogenetic control of cardiac function. *Science*. 2010;330:971–974.
- Jia Z, Lu Z, Bien H, Liu H, Rosati B, Cohen IS, Entcheva E. Optically activated light-sensitive channels can pace cardiac tissue and generate propagating cardiac impulses. *Circ Res*. 2010;107:e37.
- Valiunas V, Kanaporis G, Valiuniene L, Gordon C, Wang HZ, Li L, Robinson RB, Rosen MR, Cohen IS, Brink PR. Coupling an hcn2-expressing cell to a myocyte creates a two-cell pacing unit. *J Physiol*. 2009;587:5211–5226.
- Chung CY, Bien H, Entcheva E. The role of cardiac tissue alignment in modulating electrical function. *J Cardiovasc Electrophysiol*. 2007;18:1323–1329.
- Entcheva E, Bien H. Macroscopic optical mapping of excitation in cardiac cell networks with ultra-high spatiotemporal resolution. *Prog Biophys Mol Biol*. 2006;92:232–257.
- Bien H, Yin L, Entcheva E. Calcium instabilities in mammalian cardiomyocyte networks. *Biophys J*. 2006;90:2628–2640.
- Chater TE, Henley JM, Brown JT, Randall AD. Voltage- and temperature-dependent gating of heterologously expressed channelrhodopsin-2. *J Neurosci Methods*. 2010;193:7–13.
- Malmivuo J, Plonsey R. *Bioelectromagnetism*. Chapter 3. New York: Oxford University Press; 1995.
- Cardin JA, Carlen M, Meletis K, Knoblich U, Zhang F, Deisseroth K, Tsai LH, Moore CI. Targeted optogenetic stimulation and recording of neurons in vivo using cell-type-specific expression of channelrhodopsin-2. *Nat Protoc*. 2010;5:247–254.
- Plotnikov AN, Shlapakova I, Szabolcs MJ, Danilo P Jr, Lorell BH, Potapova IA, Lu Z, Rosen AB, Mathias RT, Brink PR, Robinson RB, Cohen IS, Rosen MR. Xenografted adult human mesenchymal stem cells provide a platform for sustained biological pacemaker function in canine heart. *Circulation*. 2007;116:706–713.
- Potapova I, Plotnikov A, Lu Z, Danilo P Jr, Valiunas V, Qu J, Doronin S, Zuckerman J, Shlapakova IN, Gao J, Pan Z, Herron AJ, Robinson RB, Brink PR, Rosen MR, Cohen IS. Human mesenchymal stem cells as a gene delivery system to create cardiac pacemakers. *Circ Res*. 2004;94:952–959.
- Rushton WAH. Initiation of the propagated disturbance. *Proc R Soc Lond B*. 1937;124:210–243.
- Fozzard HA, Schoenberg M. Strength-duration curves in cardiac Purkinje fibres: effects of liminal length and charge distribution. *J Physiol*. 1972;226:593–618.
- Xie Y, Sato D, Garfinkel A, Qu Z, Weiss JN. So little source, so much sink: requirements for afterdepolarizations to propagate in tissue. *Biophys J*. 2010;99:1408–1415.
- Han X, Qian X, Bernstein JG, Zhou HH, Franzesi GT, Stern P, Bronson RT, Graybiel AM, Desimone R, Boyden ES. Millisecond-timescale optical control of neural dynamics in the nonhuman primate brain. *Neuron*. 2009;62:191–198.

### CLINICAL PERSPECTIVE

Recently, basic research in neuroscience has been revolutionized by the use of cloned light-sensitive ion channels, originally found in microorganisms, for precise spatiotemporal perturbation and control of neurons in different parts of the brain. The potential of this new approach, termed optogenetics, is being explored for clinical use in deep brain stimulation. In the present study, we demonstrate the utility of optogenetics for pacing of cardiac muscle. We show that a cell delivery strategy can be used to inscribe light-sensitivity in cardiac tissue. Nonexcitable cells, for example, autologous cells from a patient, can potentially be induced to express such light-sensitive ion channels (Channelrhodopsin-2) that provide robust depolarizing current on light stimulation. When electrically coupled to the surrounding cardiomyocytes, the delivered cells can produce optically excitable heart tissue. We validated this approach in a 2-dimensional in vitro syncytium and show that the triggered excitation waves by electric pacing and by optical pacing have identical properties and that the genetic modification does not adversely alter the electrophysiology of the cardiac tissue. Our results demonstrate feasibility to control excitation and contraction in cardiac muscle by light. Because optical pacing in this case uses less energy and offers superior spatiotemporal control and remote access, we believe that it can serve not only as an elegant tool in arrhythmia research but may form the basis for a new generation of light-driven cardiac pacemakers and muscle actuators.

## **SUPPLEMENTAL MATERIAL**

### **I. Detailed Methods**

### **II. Supplementary Figures (2)**

### **III. Supplementary Movies (4)**

### **IV. Equivalent Circuit Analysis of TCUs**

## **I. DETAILED METHODS**

### **Development of a ChR2-expressing stable cell line**

A bacterial stock containing the pcDNA3.1/hChR2(H134R)-EYFP plasmid was obtained from Addgene and amplified in selective Luria-Bertani (LB) medium. Plasmid DNA was extracted using Qiagen HiSpeed Plasmid kit (Qiagen, Valencia, CA), ethanol-precipitated and resuspended in endotoxin-free water for use in cell transfections. After verification of identity by restriction digestion and sequencing, it was stored at -20°C at the obtained concentration (typically 2-4 µg/ml), later diluted to 1 µg/ml for transfection.

HEK293 cells (ATCC, Manassas, VA) were transfected with the plasmid using Lipofectamine™ 2000 (Invitrogen) as directed: 4 µg of DNA and 10 µg of Lipofectamine in 250 µl medium for a 35mm dish with cells. Gene expression was examined by EYFP signal the next day. 48 hours after transfection, cells were switched to selection medium, containing 500 µg/ml Geneticin (GIBCO Invitrogen). The selected cells with a high fluorescence signal were maintained in Geneticin (500 µg/ml) containing culture medium at 37° in a humidified atmosphere incubator with 5% CO<sub>2</sub> and 95% air. Expanded HEK cell cultures showing near 100% expression were frozen at -80C for later use. Immediately prior to use, the HEK-ChR2 cells were grown in DMEM

(Dulbecco's Modified Eagle's Medium, GIBCO Invitrogen) supplemented with 10% FBS (fetal bovine serum, Sigma-Aldrich, St Louis, MO) and 1% penicillin-streptomycin (Sigma) at 37°, 5% CO<sub>2</sub>. Expression and functional properties were confirmed in passages 2 to 20 and used in co-culture experiments with cardiomyocytes.

### **Confirmation and analysis of light-triggered ChR2-current in the cell delivery system**

ChR2 cell membrane expression was confirmed in virtually 100% of the transfected HEK cells (**Fig. 2b**) using EYFP fluorescence as a marker. For functional measurements of the ChR2-current, the HEK-ChR2 cells were harvested by trypsinization, replated at low density on polylysine-coated coverslips and stored in DMEM medium at 37° in a humidified atmosphere incubator with 5% CO<sub>2</sub>. The membrane current was recorded in single cell by whole-cell patch clamp with an Axopatch 1D amplifier (Axon instruments Inc, Foster City, CA). Borosilicate glass pipettes (World Precision Instruments Inc., Sarasota, FL) were pulled on a Flaming-Brown-type pipette puller (Sutter Instrument Co, Novato, CA) and heat-polished before use. Pipette resistances measured in Tyrode's solution were 3-4 MΩ when filled with pipette solution. The pipette solution contained (mmol/L) potassium aspartate 80, KCl 50, MgCl<sub>2</sub> 1, MgATP 3, EGTA 10 and HEPES 10 (pH 7.4 with KOH). The external solution contained (mmol/L) KCl 5.4, NaCl 140, MgCl<sub>2</sub> 1, CaCl<sub>2</sub> 1.8, HEPES 10 and Glucose 10 (pH 7.4 with NaOH). Membrane currents were recorded, digitized (DIGIDATA 1320A, Axon Instruments) and stored for offline analysis. There was a liquid junction potential of ~10 mV between the bath solutions and the electrode solution. The current was recorded as depolarizing 500ms pulses from -80 mV to +50mV with and without illumination (**Fig. 2**). The light-triggered ChR2-current was determined by subtracting the "off" light trace from the recorded response of light "on". Illumination pulses were generated using the microscope-attached fluorescence light unit, filtered at 470nm. The light-triggered inward ChR2-current was reproducible upon repeated on/off light pulses.

The kinetics of light-triggered ChR2-current was examined as the cells were clamped at -80mV after obtaining whole-cell configuration, and light pulses of variable duration and spacing were applied sequentially. For the analysis of the current kinetics – activation and deactivation time-constants - nonlinear sigmoidal curve fit was applied to the rising and the falling portion upon light on/off pulse (**Fig. 2d-e**). The slope parameter ( $\tau_{sl}$ ) was quantified.

### **Optically-excitabile cardiac syncytium: primary cardiomyocyte cell culture and co-culture with HEK-ChR2 cells**

Neonatal Sprague-Dawley rats were sacrificed and cardiomyocytes were isolated by an approved Stony Brook University IACUC protocol as previously described<sup>1-5</sup>. Briefly, the ventricular portion of the hearts was excised and washed free of blood. The tissue was cut into small pieces and enzymatically digested overnight with trypsin at 4° (1mg/ml, USB, Cleveland, OH), and then with collagenase at 37° (1mg/ml, Worthington, Lakewood, NJ) the next morning. Cardiac fibroblasts were removed by a two-stage pre-plating process. In some transfection experiments, these cardiac fibroblasts were used in conjunction with electroporation.

Cardiomyocytes were then plated onto fibronectin-coated glass coverslips at high density:  $4 \times 10^5$  cells/cm<sup>2</sup> for the control myocyte group and  $3.5 \times 10^5$  cells/cm<sup>2</sup> for the co-culture groups, mixed with approximately 7,700 or 3,500 HEK cells (for 45:1 and 100:1 initial plating ratios) onto glass bottom dishes in M199 medium (GIBCO Invitrogen) supplemented with 10% fetal bovine serum (GIBCO Invitrogen) for the first 2 days and then reduced to 2%. Cultures were maintained in an incubator at 37° with 5% CO<sub>2</sub> for 4 to 5 days before functional measurements.

### **Direct expression of ChR2-EYFP in cardiomyocytes, cardiac fibroblasts and mesenchymal stem cells**

Freshly isolated neonatal rat cardiomyocytes and cardiac fibroblasts, as well as mesenchymal stem cells, were transfected by electroporation using a Nucleofector device (Amaxa Lonza, Gaithersburg, MD) as follows: 4 µg of plasmid DNA was mixed with 100 µl of nucleofector solution for transfecting  $4 \times 10^6$  cells. Human mesenchymal stem cells (hMSC) were purchased from Clonetics/BioWhittaker, Walkersville, MD, USA, and cultured in mesenchymal stem cell growth medium - Poietics-MSCGM (BioWhittaker). Canine mesenchymal stem cells (cMSC) were isolated from the bone marrow of adult dogs and cultured in Poietics-MSCGM. Flow cytometry revealed 93.9% CD44<sup>+</sup> and 6.1% cells were CD34<sup>+</sup>. Cells with spindle-like morphology were selected after flow cytometry characterization and replated for use. Transfected cells were incubated in normal culture conditions. Similar conditions were used to transfect cardiac fibroblasts or stem cells via electroporation. Expression of fluorescence was detected 24 to 48 hours after transfection using confocal fluorescence imaging.

Images were processed as follows: background fluorescence was first subtracted for images of control (non-transfected) and transfected cells of the same type. Then the remaining integral fluorescence over identical areas was used to form a ratio (transfected/average control) in order to quantify and compare different cell types, see **Suppl. Fig 1**.

### **Demonstration of TCU functionality in cell pairs of adult canine ventricular myocytes and HEK-ChR2**

Adult mongrel dogs were euthanized as per IACUC protocol at Stony Brook University by intravenous injection of sodium pentobarbitone (80mg/kg body weight) and the heart was removed. Canine ventricular cells were isolated using a modified Langendorff procedure<sup>6</sup>

perfusing a wedge of the left ventricle through a coronary artery with  $0.5 \text{ mg ml}^{-1}$  collagenase (Worthington) and  $0.08 \text{ mg ml}^{-1}$  protease (Sigma) for 10 min before tissue digestion. Prior to plating, isolated cardiomyocytes were stored in Kraft-Brühe (KB) solution (in mM: KCl, 83;  $\text{K}_2\text{HPO}_4$ , 30;  $\text{MgSO}_4$ , 5; Na-Pyruvic Acid, 5;  $\beta$ -OH-Butyric Acid, 5; Creatine, 5; Taurine, 20; Glucose, 10; EGTA, 0.5; KOH, 2; and  $\text{Na}_2\text{-ATP}$ , 5; pH was adjusted to 7.2 with KOH) at room temperature. The canine ventricular myocytes were plated onto laminin-coated glass coverslips ( $10 \text{ }\mu\text{g/ml}$ , Invitrogen) and incubated in a  $37^\circ\text{C}$  to ensure attachment. HEK-ChR2 cells were added within 24h at low density to stimulate formation of individual cell pairs and the co-culture was maintained in Medium 199 (Gibco) supplemented with 15% FBS, 2 mm l-glutamine,  $100 \text{ U ml}^{-1}$  penicillin,  $100 \text{ }\mu\text{g ml}^{-1}$  streptomycin and  $50 \text{ }\mu\text{g ml}^{-1}$  gentamicin.

Dual patch clamp experiments were performed within 48 hours after plating. Briefly, experiments were carried out on heterologous (HEK-ChR2 - canine myocyte) cell pairs within 48 hours after plating, as described previously<sup>7</sup>. A dual whole-cell voltage-clamp method was used to control and record the membrane potential of both cells and to measure associated membrane and junctional currents<sup>7-9</sup>. Each cell of a pair was voltage clamped at the same potential by two separate patch clamp amplifiers (Axopatch 200, Axon Instruments). To record junctional conductance, brief voltage steps ( $\pm 10 \text{ mV}$ , 400 ms) were applied to one cell of a pair, whereas the other cell was held at constant voltage and the junctional currents were recorded from the unstepped cell. Membrane and action potentials were recorded in current-clamp mode.

For electrical recordings, glass coverslips with adherent cells were transferred to an experimental chamber mounted on the stage of an inverted microscope (Olympus-IX71) equipped with a fluorescence imaging system. The chamber was perfused at room temperature ( $\sim 22^\circ\text{C}$ ) with bath solution containing (in mM): NaCl, 140;  $\text{Mg Cl}_2$ , 1; KCl, 5;  $\text{CaCl}_2$ , 2; HEPES, 5 (pH 7.4); glucose, 10. Perfusion with  $200 \text{ }\mu\text{M}$  of carbenoxolone (Sigma) was used to block cell-cell communication. The patch pipettes were filled with solution containing (in mM):  $\text{K}^+$

aspartate<sup>-</sup>, 120; NaCl, 10; MgATP, 3; HEPES, 5 (pH 7.2); EGTA, 10 (pCa ~8). Patch pipettes were pulled from glass capillaries (code GC150F-10; Harvard Apparatus) with a horizontal puller (DMZ-Universal, Zeitz-Instrumente). When filled, the resistance of the pipettes measured 1-4M  $\Omega$ .

### **Immunostaining of co-cultures**

For immunocytochemistry, the co-cultures were fixed and permeabilized with 3.7% formaldehyde and 0.02% Triton-X 100 before being stained with a monoclonal mouse antibody against sarcomeric  $\alpha$ -actinin (Sigma). Samples were visualized using goat anti-mouse antibody conjugated with fluorophore Alexa 546 (Invitrogen) and imaged on the Olympus FluoView confocal system.

### **Western blots of Cx43 and $\alpha$ -tubulin**

Cells from three groups (HEK293, HEK+ChR2 and stably transfected HeLa+Cx43 cells) were collected, lysed and centrifuged to obtain a pellet. The pellets were re-suspended in cold RIPA buffer (R0278, Sigma), protease Inhibitor cocktail (P2714, Sigma), sodium orthovanadate (S-6508, Sigma) and PMSF (P-7626, Sigma); after centrifugation, the supernatants were transferred to pre chilled microtubes. Protein concentration for each sample was determined by the Bradford assay. Total protein of 30 micrograms from each lysate was mixed with equal volume of laemmli sample buffer (161-0737, Bio-Rad, Hercules, CA) containing  $\beta$ -mercaptoethanol and boiled for 5 minutes at 95°C. After centrifugation, samples were loaded on a SDS-polacrylamide gel. MagicMark XP Protein Standard (LC5602, Invitrogen) was loaded along with the samples. After separation by electrophoresis at 115 V for 90 minutes in tris-glycine/SDS buffer, proteins were transferred to immobilon-P membrane (Millipore, Billerica, MA) by electrophoresis at 100 V for 60 minutes in tris-glycine/methanol buffer. Nonspecific

antibody binding was blocked for 1 hour by 5% blotting grade blocker non-fat dry milk (Bio-Rad) dissolved in 1x TBST. The following antibodies were used: primary anti-Cx43 antibody raised in rabbit (C 6219, Sigma), secondary goat-anti-rabbit antibody (sc-2004, Santa Cruz); a primary antibody for  $\alpha$ -tubulin at 55kD (sc-8035, Santa Cruz), and a secondary goat-anti-mouse antibody for tubulin from Pierce, Rockford, IL. The secondary antibodies were detected using SuperSignal West Femto Maximum Sensitivity Substrate (34095, Pierce) and images obtained by exposing the membrane to HyBlot CL autoradiography film. Quantification of the Cx43 bands relative to the  $\alpha$ -tubulin bands was done using a built-in routine in ImageG.

### **Ultra-high resolution optical mapping of cardiac excitation waves triggered by light in co-cultures**

Two-dimensional optical mapping over a large field of view (about 2.2cm) was done with a custom-developed macroscopic system allowing for ultra-high spatiotemporal resolution<sup>4,5</sup>. The system (**Fig. 4a**) includes a CMOS camera (pco, Germany) recording images at 200 frames per second (fps) over 1,280×1,024 pixels), a Gen III fast-response intensifier (Video Scope International, Dulles, VA), collecting optics (Navitar Platinum lens, 50mm, f/1.0) and filters, excitation light source (Oriel with fiber optics light guides) and an adjustable imaging stage. Subcellular spatial resolution was achieved – about 22  $\mu$ m per pixel. All measurements were done in normal Tyrode's solution at room temperature. Quest Rhod-4 (AAT Bioquest, Sunnyvale, CA) was used to label the cells for tracking  $\text{Ca}^{2+}$  waves. This optical dye was chosen for wavelength compatibility with ChR2 and EYFP excitations/emissions. Excitation light (525nm) for  $\text{Ca}^{2+}$  recording was delivered through non-conventional distributed tangential illumination (90° angle with respect to the optical axis) to accommodate optical stimulation but also to achieve superior contrast by complete uncoupling of the Rhod-4 excitation from the light-gathering optics, **Fig. 4a**. Excitation light for Rhod-4 was provided by a QTH lamp with a



branching liquid light guide, attached to a custom designed experimental chamber with reflective inner walls and open bottom surface, accommodating a 35mm dish with the sample. Emitted Rhod-4 fluorescence was collected at 585nm through an emission filter in front of the intensified camera on top of the sample.

All movies of propagation were acquired using CamWare (pco, Germany) data acquisition software. Raw data were binned (2×2) and analyzed in custom-developed Matlab software to extract quantitative information about calcium transient morphology, conduction velocity etc. Activation maps (based on time of maximum rise in Ca<sup>2+</sup>) and phase movies (using the Hilbert transform) were generated after filtering spatially (Bartlett filter, 5-pixel kernel) and temporally (Savitsky-Golay, order 2, width 7)<sup>3, 5</sup>.

### **Electrical and optical pacing**

For records of electrically-triggered activity, cells were paced by Pt electrodes, connected to a computer-driven Myopacer stimulator (IonOptix, Milton, MA). Excitation pulses for light-triggered activity were delivered through the bottom of the dish from an optically focused light from an LED (470nm, 1.35 cd, 20mA, 5mm, 30deg angle) from Optek Technology (Carrollton, TX) or from a fiber-optics coupled high-power blue LED (470nm, 1.6A), Thor Labs (Newton, NJ), connected to the TTL output of a second computer-driven Myopacer stimulator. Irradiance (in mW/mm<sup>2</sup>) was measured at the cell monolayer site using a Newport digital optical power meter Model 815 (Newport, Irvine, CA), with a sensor area of 0.4cm×0.4cm, with wavelength set at 470nm. Values are reported for each experiment.

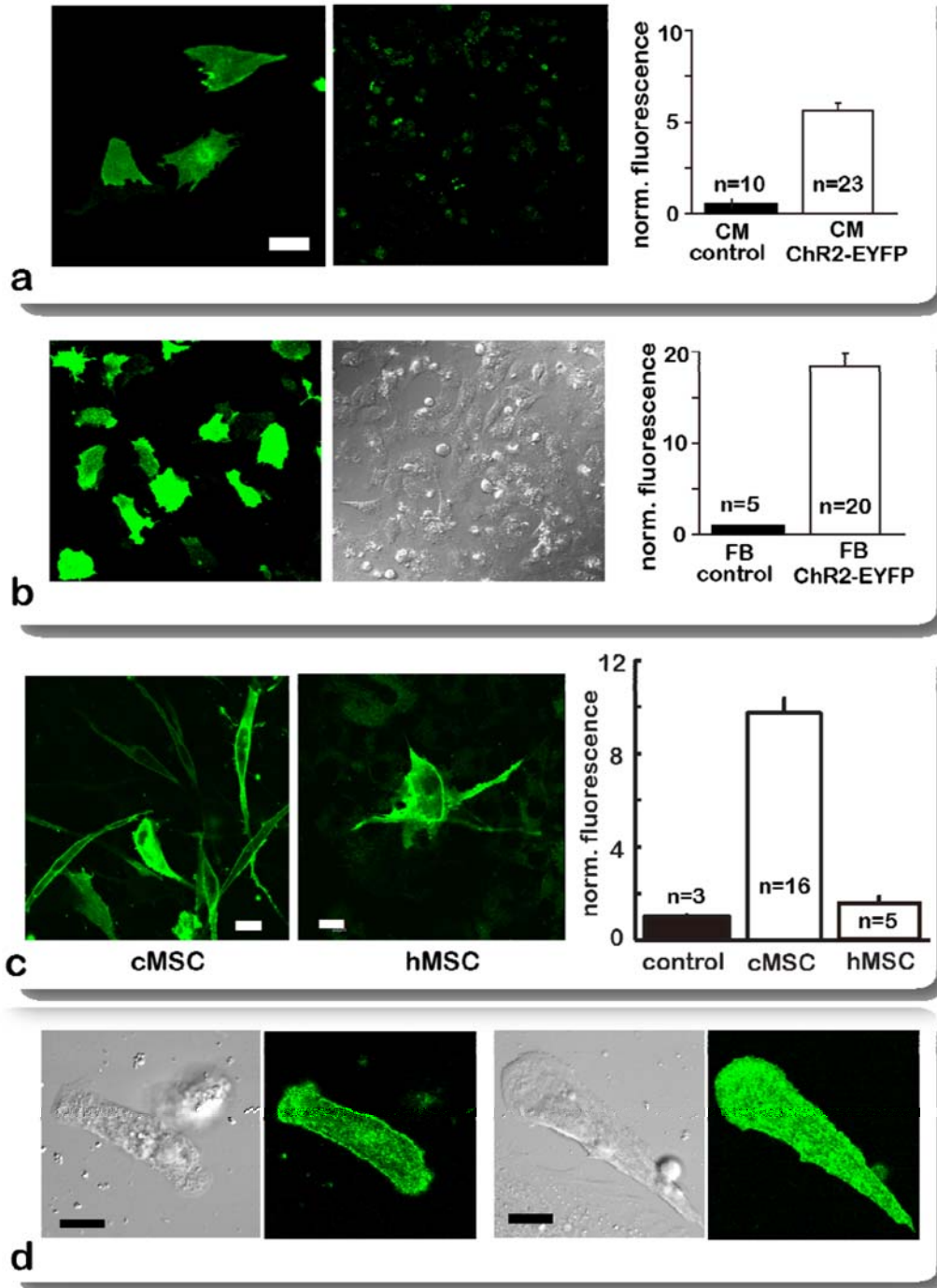
### **Recording light-triggered contractions**

Microscopic imaging for confirmation of gene expression or for documenting contractions by optical excitation was done with the Olympus FluoView™ FV1000 confocal system at room temperature. Hamamatsu ImagEM EMCCD camera (Hamamatsu, Bridgewater, NJ), attached to the Olympus FluoView™ FV1000 microscope, was used to record contractility movies at 20 fps with a 60X oil lens (NA=1.42), using SlideBook 5 software (Intelligent Imaging Innovations, Denver, CO). In addition, contractility response was also documented by automatic optical tracking of cell length<sup>1</sup> at 250Hz using an IonOptix videosystem (IonOptix) attached to a Nikon TE2000 inverted microscope.

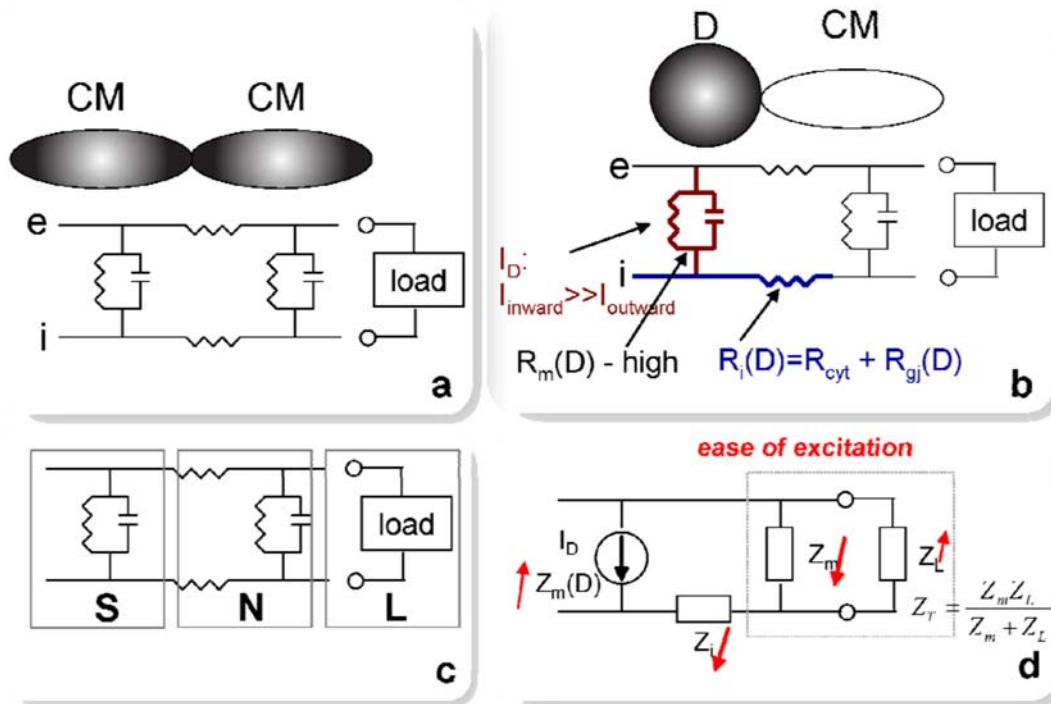
#### **Carbenoxolone treatment to test effects of cell coupling on TCU**

Carbenoxolone, CBX, (Sigma), a gap junctional uncoupler<sup>8</sup>, was used at a concentration 200 $\mu$ M in the dual-patch experiments with canine CM and HEK-ChR2 or in the cardiac syncytium of neonatal rat CM and HEK-ChR2. In the latter case, CBX was applied for 20min (without perfusion) in the co-cultures of HEK-ChR2 cells and cardiomyocytes. Contractility movies were recorded in response to optical pacing before and during administration of carbenoxolone, and upon washout to assess the role of gap junctional coupling in the functionality of the TCU.

## II. Supplementary Figures



**Supplementary Figure 1. Direct expression of light-sensitive channels in cardiac cells and mesenchymal stem cells via electroporation.** **a:** Cardiac myocytes express ChR2-EYFP at low efficiency after electroporation (left), control (right); scale bar is 50 $\mu$ m. Panel **b:** Cardiac fibroblasts robustly express ChR2 after electroporation. **c:** Expression of ChR2 in mesenchymal stem cells – canine (cMSC) and human (hMSC). cMSC showed substantially better expression than hMSC. Scale bar is 20 $\mu$ m. Data in the bar graphs are mean $\pm$ SEM. Normalized fluorescence is the image's total fluorescence normalized by the mean fluorescence from control (non-transfected) cells of the same type. **d:** Phase and fluorescence (EYFP) images of two electroporation-transfected cardiomyocytes, for which movies of optically-triggered contractions are provided. Scale bar is 20 $\mu$ m.



**Supplementary Figure 2. Equivalent circuit for TCU-mediated excitation of cardiac tissue. a:** CM-CM cell pair where both cell carry the excitatory current, and equivalent circuit. **b:** TCU of a donor (D) cell and a CM, with differences listed. **c:** abstraction using a Source-Neighbor-Load (S-N-L) triad for a spatially-extended system. **d:** simplified equivalent circuit of the S-N-L; red arrows indicate the direction of contribution of the different circuit elements towards "ease of excitation", as analyzed below.

### **III. Supplementary Movies**

#### **Supplementary Movie 1: CM-only ChR2 contractions (compressed)**

Shown are two examples of contractions in optically-paced neonatal rat cardiomyocytes, directly transfected with ChR2-EYFP by electroporation using nucleofector technology. ChR2 expression was firstly confirmed using Olympus FluoView™ FV1000 confocal microscope, as shown in the still fluorescence image before each contractility movie: green shows the reporter gene EYFP. Contractility was recorded at 20 fps using an EMCCD camera with 60X oil lens (NA=1.42). Optical stimulation was achieved by switching on/off blue light (470nm), easily seen by the brightness in the field of view and the lightening up of the cardiomyocytes during pacing pulses. The black scale bar in the contractility movie is 10µm.

#### **Supplementary Movie 2: CM-HEK pair coupling test (carbenoxolone)**

The role of gap junctional coupling in forming a “tandem cell unit” that responds to light was tested here. This is a sparse co-culture of HEK-ChR2-EYFP and neonatal rat cardiomyocytes (CM). The movie shows optical excitation (and resulting CM contraction) before and during treatment with an uncoupling agent – carbenoxolone (200µM, 20min) and after washout of the drug. Contractility was recorded at 20 fps using an EMCCD camera with 60X oil lens (NA=1.42). Optical stimulation was achieved by switching on/off blue light (470nm), easily seen by the brightness in the field of view and the lightening up of the HEK cells during pacing pulses. The black scale bar in the contractility movie is 10µm.

#### **Supplementary Movie 3: CM+HEK-contractions-optical stimulation-confocal**

The movie shows two examples of contractions in optically-paced cardiac tissue (room temperature), in which neonatal rat cardiomyocytes were co-cultured with ChR2-expressing HEK cells at initial ratio of 45:1. Movie was recorded at 20 fps using an EMCCD camera with 60X oil lens (NA=1.42), attached to an Olympus FluoView™ FV1000 microscope. Optical stimulation was achieved by switching on/off blue light (470nm), easily seen by the brightness in

the field of view and the lighting up of the HEK cells during pacing pulses (due to some wavelength overlap with excitation of the reporter gene EYFP). Scale bar in the movie is 10 $\mu$ m.

**Supplementary Movie 4: Optical mapping of propagation in CM+HEK+ChR2-3.4 speed**

Electrical pacing and all-optical interrogation of cardiac tissue are shown (room temperature, 45:1 initial mixing ratio). Ca<sup>2+</sup> wave propagation in cardiac tissue, in which neonatal rat cardiomyocytes were co-cultured with ChR2-expressing HEK cells, was done with Rhod-4. In the top panels, blue line shows the timing of electrical stimulation (in this case – a line Pt electrode on the left) or optical stimulation from a blue LED (470nm),: 0 is “off”, 1 is “on”. The black trace is the corresponding Ca<sup>2+</sup> transient from a pixel in the image (indicated by “\*” in the bottom panel). The bottom panels show color-coded (Hilbert) phase movies of Ca<sup>2+</sup> wave propagation acquired by our custom-developed ultra-high resolution macroscopic system and processed in Matlab (color indicates phase during a cycle, black line denotes the wave-front; details are given in the Methods section). Movie is played at  $\frac{3}{4}$  real speed. The scale bar in the movie is 2mm.

## IV. Equivalent Circuit Analysis of TCU

When comparing the TCU strategy to direct expression of ChR2 in the native myocytes (mostly by viral methods), several important differences are worth mentioning, **Supplementary Fig 2**: (1) the donor (D) cells are non-excitabile and typically do not have major repolarizing currents, i.e. the ChR2 inward current is their main current, unlike native CMs; (2) the D-cells have higher membrane impedance at rest due to smaller/negligible inward rectifier,  $I_{K1}$ , and typically have a more depolarized resting potential; (3) compared to CM-CM coupling, the D-CM coupling is typically somewhat reduced. We ask the question: What factors in the TCU approach affect the ease of excitation and how is the TCU response different than the response of a homogeneous myocardial tissue with direct expression of ChR2?

For a spatially-extended tissue, when the cell pair (TCU) is connected to some “load” of excitable cells (CMs), the system can be abstracted to a Source-Neighbor-Load (S-N-L) triad for easier analysis. A simplified equivalent circuit of such a triad is presented in **Supplementary Fig 2d**, derived under the following assumptions: use of equivalent impedances ( $Z$ ); assuming negligibly small extracellular impedance  $Z_e$ ; for the immediate neighbor cells to be charged (N), we consider the membrane  $Z_m$  and intracellular (coupling) impedance  $Z_i$ , but for the rest of the tissue – consider a lumped/load impedance,  $Z_L$ . Red arrows indicated the direction of contribution of the different circuit elements towards “ease of excitation”, as analyzed below.

For the simplified circuit in **Supplementary Fig 2d**, we can derive the following expressions, representing the underlying current-divider circuits and the total current drawn by the circuit,  $I_T$ , as well as the current to excite the immediate neighbors, i.e. the current of interest,  $I_m$ :

$$I_T = \frac{Z_m(D)}{Z_i + Z_T} I_D \quad (1)$$

$$I_m = \frac{Z_L}{Z_m + Z_L} I_T \quad (2)$$



We want to determine how the elements of the circuit determine the “**ease of excitation**” of the system, i.e. what fraction of  $I_D$  does  $I_m$  constitute? Our simplified analysis only considers steady-state passive response and ignores the kinetics of the ion channels and/or transient processes, which are admittedly very important.

The following observations can be made:

- 1) Higher  $Z_m$  for the source, i.e.  $Z_m(D) > Z_m(CM)$ , makes the source closer to an “ideal current source” (with infinite internal resistance/impedance) and therefore increases the “ease of excitation”, i.e. for a given light-induced  $I_D$ , more current  $I_m$  will be available for excitation of the neighbors in the TCU case, which follows directly from Eqn 1.
- 2) Higher load, i.e. low  $Z_L$ , such that  $Z_m \gg Z_L$ , and  $Z_T \approx Z_L \rightarrow 0$ , that may occur in very well-coupled, spatially-extended tissue (higher dimensionality) will indeed make it harder to excite by making  $I_m$  a smaller fraction of  $I_D$  – see simplified combination of Eqns 1 and 2 for this case:

$$I_m = \frac{Z_m(D)}{Z_i} \frac{Z_L}{Z_m} I_D \quad (3)$$

- 3) Very low load, i.e. high  $Z_L$ , such that  $Z_L > Z_m$ , and  $Z_T \approx Z_m$ ) applies for small cell clusters and/or highly uncoupled tissue, and highlights the importance of the coupling to the immediate neighbors,  $Z_i$  and the membrane impedance of the immediate neighbors. The ease of excitation will improve by higher coupling to the neighbors for CM-CM (low  $Z_i$ ) in this case compared to D-CM and lower  $Z_m$  of the neighbors (possibly determined by the equivalent  $K^+$  conductance in the neighbor CMs), as seen from the simplified Eqn. 4.

$$I_m = \frac{Z_m(D)}{Z_i + Z_m} I_D \quad (4)$$

- 4) Overall, better coupling for S-N, but reduced coupling (and equivalent conductivity) for N-L works towards ease of excitation. It is important to note, however, that for spatially distributed D-cells, the S-N coupling in the S-N-L triad plays a dual role, i.e. it affects both the S-N charge transfer and the equivalent “load” presented by the tissue. All parameters indicated in **d** act in parallel and actual simulations, quantification is needed to fully uncover the extent of their individual contribution.

## REFERENCES

1. Entcheva E, Bien H. Tension development and nuclear eccentricity in topographically controlled cardiac syncytium. *J Biomed Microdev.* 2003;5:163-168
2. Yin L, Bien H, Entcheva E. Scaffold topography alters intracellular calcium dynamics in cultured cardiomyocyte networks. *Am J Physiol Heart Circ Physiol.* 2004;287:H1276-H1285
3. Chung CY, Bien H, Entcheva E. The role of cardiac tissue alignment in modulating electrical function. *J Cardiovasc Electrophysiol.* 2007;18:1323-1329
4. Entcheva E, Bien H. Macroscopic optical mapping of excitation in cardiac cell networks with ultra-high spatiotemporal resolution. *Prog.Biophys.Mol.Biol.* 2006;92:232-257
5. Bien H, Yin L, Entcheva E. Calcium instabilities in mammalian cardiomyocyte networks. *Biophys.J.* 2006;90:2628-2640
6. Yu H, Gao J, Wang H, Wymore R, Steinberg S, McKinnon D, Rosen MR, Cohen IS. Effects of the renin-angiotensin system on the current  $i_{to}$  in epicardial and endocardial ventricular myocytes from the canine heart. *Circ Res.* 2000;86:1062-1068
7. Valiunas V, Kanaporis G, Valiuniene L, Gordon C, Wang HZ, Li L, Robinson RB, Rosen MR, Cohen IS, Brink PR. Coupling an hcn2-expressing cell to a myocyte creates a two-cell pacing unit. *J Physiol.* 2009;587:5211-5226
8. Valiunas V, Kanaporis G, Valiuniene L, Gordon C, Wang H, Li L, Robinson RB, Rosen MR, Cohen IS, Brink PR. Coupling an hcn2 expressing cell to a myocyte creates a two cell pacing unit. *J Physiol.* 2009
9. Valiunas V, Beyer EC, Brink PR. Cardiac gap junction channels show quantitative differences in selectivity. *Circ.Res.* 2002;91:104-111